Decay channels of the discrete and continuum Xe 4*d* resonances

U. Becker
Institut für Strahlungs- und Kernphysik, Technische Universität Berlin, D-1000 Berlin 12, Federal Republic of Germany

T. Prescher, E. Schmidt,* B. Sonntag, and H. -E. Wetzel
II. Institut für Experimentalphysik der Universität Hamburg, D-2000 Hamburg 50, Federal Republic of Germany

(Received 23 December 1985)

Excitations of the Xe 4*d* subshell to discrete *np* and continuum ϵf states have been studied by photoemission. The resonant photoelectron spectra provide the first direct evidence that the emission of continuously distributed shakeoff electrons is one of the dominant decay modes of the $4d \rightarrow np$ resonances. The same effect is proposed to account for the missing 4*d* intensity in the $4d \rightarrow \epsilon f$ shape resonance compared to the absorption cross section. The fraction of direct recombination in the decay of the $4d \rightarrow np$ resonances was determined quantitatively by partial cross-section and branching-ratio measurements of the 5*s* and 5*p* main lines in the photon-energy range from 60 to 70 eV. The modified Fano theory for partial cross sections was applied to nearly Lorentzian-type profiles in order to derive partial decay widths. The decay into the 5*s* and 5*p* photoemission channels amounts to less than 0.5% of the total decay rate. The $5p_{3/2}$:$5p_{1/2}$ branching ratio was measured over a broad range (17–140 eV) in order to test details of relativistic random-phase approximation calculations concerning intershell correlations between the 4*d* and 5*p* subshells.

I. INTRODUCTION

Excitations of the Xe 4*d* subshell have attracted continuous interest during the last decades (see, e.g, Refs. 1–3 and references therein). Xe played, and still plays, a key role in the elucidation of such basic phenomena as, e.g., delayed onset, atomic shape resonances,[4,5] interchannel coupling, satellites, and threshold effects. The Xe 4*d* excitations display both series of strong discrete $4d \rightarrow np$ resonances below threshold and a prominent $4d \rightarrow \epsilon f$ atomic shape resonance above threshold. The suppression of $4d \rightarrow nf$ resonances and the existence of the shape resonance result from a repulsive barrier of the effective potential. The decay of the discrete and the continuum resonances forms the focus of our study. The main questions addressed are the following: (i) How strongly do shakeoff processes participate? (ii) What is the contribution of direct recombination or, in other words, how much autoionization into the 5*p* and 5*s* continua is present?

Previous investigations, limited by low-energy resolution and low count rates, could only in part answer these questions. In order to obtain better qualitative and quantitative answers we reexamined the Xe photoelectron spectra for photon energies between 25 and 160 eV with special emphasis on high-resolution measurements in the energy range of the discrete excitations.

II. EXPERIMENTAL

The experiment was performed with photons from beamline D4.2 at the Hamburger Synchrotronstrahlungslabor (HASYLAB) at Deutsches Elektronen-Synchrotron (DESY), which employs the 5.6-m toroidal grating monochromator.[6] The monochromator was operated with narrow slits in order to achieve a resolution of about 160 meV comparable to the natural linewidths of the $4d \rightarrow np$ excitations under study.[7] The gas sample was introduced into the experimental chamber via a capillary tube. The Xe background pressure in the chamber was about 2×10^{-4} mbar. A differential pumping stage separated the chamber from the beamline.

Photoelectrons and Auger electrons were analyzed with a cylindrical mirror-type electron spectrometer. This instrument is insensitive to the angular distribution of photoelectrons.[8] The electron spectrometer has a constant resolution of 0.74% of the kinetic energy and its transmission is directly proportional to the kinetic energy. At $h\nu=65$ eV and a typical photon flux of 10^{10} s^{-1} we obtained approximately 50 counts/s in the Xe $5p_{3/2}$ photoelectron line. The raw photoelectron spectra were corrected for the analyzer transmission function $1/E_{\rm kin}$. Also, a small background of less than 2% of the maximal intensity had to be subtracted. Figure 1 shows an example of such a corrected spectrum. Fitting Gaussian profiles to the photoelectron lines yielded the areas under the peaks which in turn were used for the determination of the branching ratios. Sample pressure changes were negligible compared to the enhancement effect in the continuum. Therefore, the 5*p* and 4*d* partial cross sections between 20 and 160 eV shown in Fig. 2 were determined from these peak areas corrected by the photon flux being measured via the photocurrent of a gold diode. The conversion of this photocurrent into photon flux was based on the gold yield reported by Gudat and Kunz.[9] The uncertainty in

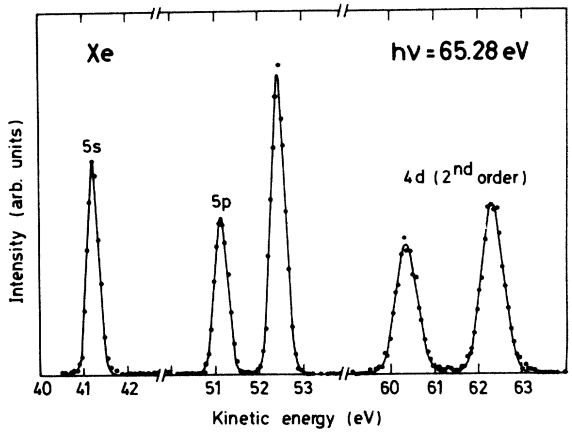

FIG. 1. $5s$, $5p$, and $4d$ (second-order light) photoelectron lines taken at a photon energy of 65.28 eV. The fitted curves are Gaussian profiles used as the instrumental function for the data analysis.

this normalization is the major problem in determining the partial cross sections. The absolute scale for these partial cross sections was established by adjusting the $5p$ cross section at 40 eV to 1.4 Mb.[10,11]

The determination of the partial cross sections in the region of the discrete $4d \rightarrow np$ resonances required an additional step of normalization. This step was necessary because the unmonitored sample pressure varied considerably during the experiment compared to the small modulations in the cross sections under study (see Fig. 7). Therefore, the $5p_{3/2}$, $5p_{1/2}$, and $5s$ intensities were normalized over the energy range of the $4d$ excitations to the second-order light-induced $4d$ intensity (see Fig. 1), which was assumed to vary smoothly with energy. The relative partial cross sections determined in this way were put on an absolute scale using the ionization-yield measurements of Hayaishi *et al.*[12] The sum of the $5p_{3/2}$, $5p_{1/2}$, and $5s$ main lines was assumed to account for the majority of the measured single-ion yield off-resonance at 63 eV.

III. RESULTS AND DISCUSSION

The discussion of the results is divided into four sections. The first addresses the importance of shakeoff processes in the range of the shape resonance. The second is concerned with the total partitioning of the decay of the $4d \rightarrow np$ excitations into different channels, while the third puts special emphasis on the contribution of direct recombination to the decay of these resonances. Because the second part required the recording of all photoelectron peaks, it is based mainly on a few spectra taken on and between the strongest resonances. The results are basically qualitative but permit us, in conjunction with previous absorption[7] and ion-yield measurements,[12] to put the evaluation of the more detailed measurements of the third section on a quantitative basis. The fourth section is concerned with the behavior of the $5p_{3/2}$:$5p_{1/2}$ branching ratio in an energy range covering both the discrete and continuum resonances. These measurements serve as a test of the quality and power of theoretical methods such as the relativistic random-phase approximation (RRPA) to describe details of the photoionization process.

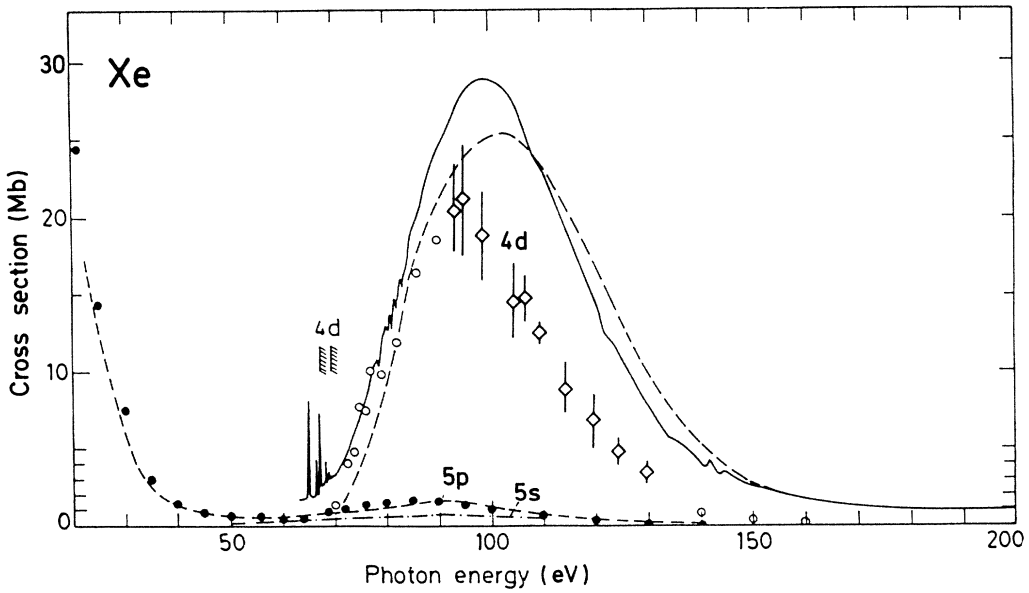

FIG. 2. Absorption cross section (Ref. 13) and the $4d$ (different sets of data: open circles, open diamonds), $5p$ (closed circles), and $5s$ (dot-dashed line representing data from Ref. 10) partial cross sections in the energy range of the $4d$ excitations. The theoretical curves (dashed line) represent RPAE calculations for the $4d$ and $5p$ cross sections by Amusia *et al.* (Ref. 15). Due to the small statistical errors the shown error bars represent only the normalization uncertainty with respect to the $5p$ cross section.

A. Shape resonance

Figure 2 shows the absorption cross section[13] in the energy range of the $4d$ excitations together with the $4d$, $5p$, and $5s$ (Ref. 10) partial cross sections. The vertical bars give the uncertainties due to the normalization to the photon flux. There are two interesting features in this figure aside from the well-known structure of the sharp $4d \rightarrow np$ excitations and the broad $4d \rightarrow \epsilon f$ shape resonance: (i) the large difference between the absorption and the $4d$ cross section above 90 eV and (ii) the intensity variation in the outer-shell $5p$ and $5s$ cross sections.

For photon energies above 90 eV the $4d$ partial cross section lies well below the total cross section. The small $5p$ and $5s$ cross sections cannot make up for the difference. The missing $4d$ intensity at the high-energy side of the shape resonance demonstrates that additional photoionization channels besides $4d$, $5p$, and $5s$ contribute considerably. Two electron channels are obvious candidates. Fahlmann *et al.*[11] have reported an enhancement of the $5s$ and $5p$ correlation satellites at the $4d$ threshold. The total cross section of all these satellites between 60 and 80 eV lies below the $5p$ cross section, and this also will hold for higher photon energies. This brings $4d$-shakeup satellites and double ionization due to shakeoff transitions into focus.[1,2,14] Unlike the corresponding case of Ba (Refs. 15 and 16) the Xe $4d$—shakeup satellites contribute less than 10%. The possible double-ionization channels in this energy region are (a) $4d^{10}5s^25p^6 \rightarrow 4d^{10}(5s+5p)^6+2e$ and (b) $4d^{10}5s^25p^6 \rightarrow 4d^9(5s+5p)^7+2e$. According to Wight and Van der Wiel[17] the cross section for outer-shell double ionization [channel (a)] is smaller than the $5p$ cross section. Therefore, the simultaneous ionization of a $4d$ and a $5p(5s)$ electron [channel (b)] accounts for most of the additional absorption. Based on atomic data[18] for Xe and Cs we estimate 90 eV for the $4d^{10}5s^25p^6 \rightarrow 4d^95s^25p^5+2e$ threshold. At this energy the partial $4d$ cross section clearly starts to fall below the total cross section. Our data are consistent with the Xe^+, Xe^{2+}, Xe^{3+}, and Xe^{4+} ion spectra reported by El-Sherbini and Van der Wiel.[19] From the Xe^{2+} and Xe^{3+} spectra these authors deduced an estimate for the strength of the $4d^{10}5s^25p^6 \rightarrow 4d^9(5s+5p)^7+2e$ channel. At 100-eV photon energy they ascribed 20% of the total absorption cross section to this double-ionization channel. Our value is close to 30% but both sets of data agree within the error limits. For the determination of the partial $4d$, $5p$, and $5s$ cross sections, West *et al.*[20] used the data of El-Sherbini and Van der Wiel[19] to correct for double ionization. Their partial cross sections thus obtained agree with ours within the error limits. Double ionization produces two electrons with a continuum of energies. With our present experimental setup it is impossible to disentangle the various double-ionization channels. But our spectra clearly show an enhancement of the low-energy electron continuum for photon energies above 90 eV. Systematic studies of this phenomenon form a challenge to both experiment and theory. The second interesting feature—the $5p$ and $5s$ enhancement in the shape resonance region—has been predicted theoretically by Amusia[21] and generally experimentally by partial cross-section measurements.[9,20] Our new set of measurements for the $5p$ cross section is in excellent agreement with calculations using the random-phase approximation with exchange (RPAE),[21] which show strong interchannel coupling among the $5p$, $5s$, and $4d$ channels. The intensity variation of the $5p$ and $5s$ cross sections is on the order of 10% of the $4d$ intensity. This is a high amplitude compared with the autoionization of the np-bound states into the same channels as shown in the following subsections.

B. Decay channels of the $4d \rightarrow np$ excitations

The decay of the Xe $4d \rightarrow 6p$ resonance has attracted considerable experimental effort since the late 1970s in order to distinguish among the different decay channels.[22–24] Most of the spectra taken for this purpose have shown the dominance of satellite enhancement [in particular, of spectator transitions (the excited electron acts as a spectator)] over autoionization into the $5p$ and $5s$ main lines, also referred to as direct recombination. But here we show for the first time the importance of resonant shakeoff processes, also referred to as resonant double-Auger processes, for the decay of the $4d \rightarrow np$ excitations. Other evidence for resonant shakeoff has been seen by scanning the energy range of the analogous Kr $3d \rightarrow np$ resonances using a zero-volt electron spectrometer.[25] Figure 3 shows the Xe photoelectron spectrum taken at the $4d \rightarrow 6p$ excitation at 65.1 eV. This spectrum has been corrected for second-order light contributions primarily due to $4d^{-1}$ Auger decay. Due to the limited detection efficiency of our analyzer at low kinetic energies, the intensity integrated over this part of the spectrum only represents a lower limit for the fractional contribution of these processes. This lower limit is consistent with the double-ionization yield of Hayaishi *et al.*[12] and measurements performed very recently at Berliner Elektronenspeicherring-Gesellschaft für Synchrotronstrahlung m.b.H (BESSY) (Berlin, Federal Republic of Germany).[26] But the spectrum shows clearly the above-mentioned contribution of continuously distributed shakeoff electrons to the decay of this resonance. The main-line contribution to the total photoelectron intensity is less than 10%, taking into account the reduced efficiency of our detector for low kinetic energies. This can be directly read off the curve in Fig. 3, giving the dispersion-corrected photoelectron intensity integrated over kinetic energy.

Figure 4 shows a principal-level scheme of Xe with excitation and decay paths of the $4d \rightarrow np$ resonances. The designation of the peaks was taken from Southworth *et al.*[18] and Becker *et al.*[26] Figure 5 shows a sequence of corrected spectra taken at several energies on (65.1, 67.0, and 68.3 eV) and between the most pronounced resonances. These spectra are in good agreement with the spectra shown by Southworth *et al.*[24] but corroborate in addition the explicit importance of shakeoff processes in the decay of the $4d \rightarrow np$ resonances. The general features of the different resonant spectra are similar. But some distinct differences can be seen—for example, the change of the intensity distribution between the $5s^25p^35d(^1P)6p$ ($E_B=46.1$ eV) and $(^3P)6p$ ($E_B=45.8$ eV) lines when raising the photon energy from 65.1 to 67.0 eV. The $5p$ and $5s$ main lines are almost unaffected by the resonances as

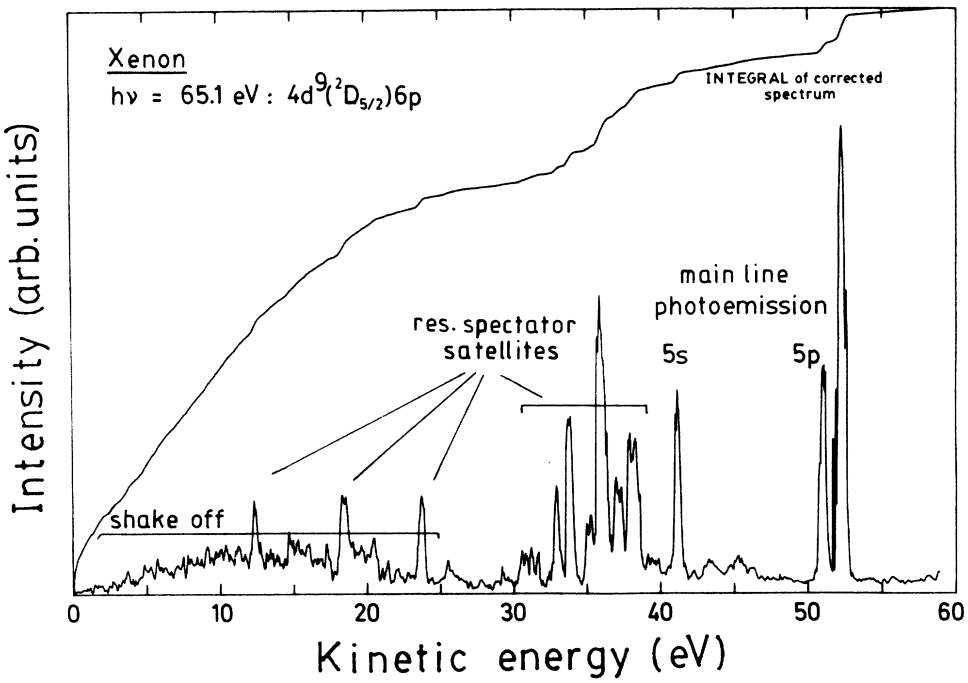

FIG. 3. Photoelectron spectrum taken at the position of the $4d \rightarrow 6p$ excitation at 65.1 eV. This spectrum has been corrected for second-order light contributions by subtraction of nonresonant $4d^{-1}$ Auger intensity. The line above the spectrum gives the dispersion-corrected intensity integrated over kinetic energy.

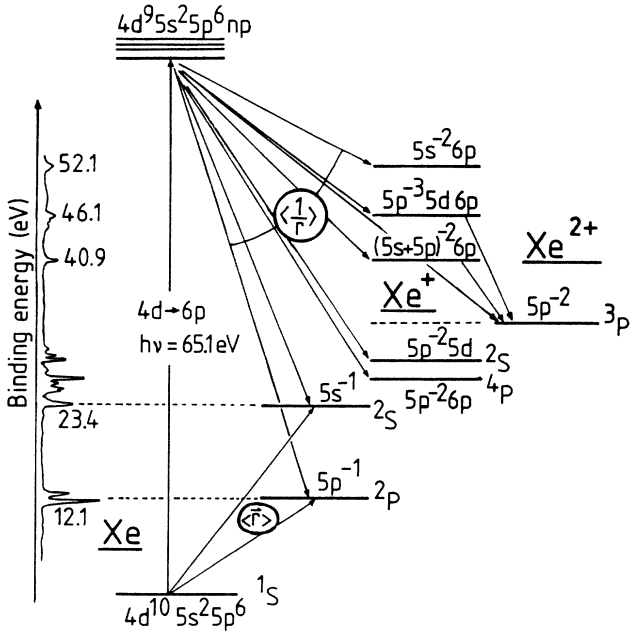

FIG. 4. Principal-level scheme of atomic Xe showing the excitation and decay paths of the $4d \rightarrow 6p$ resonance.

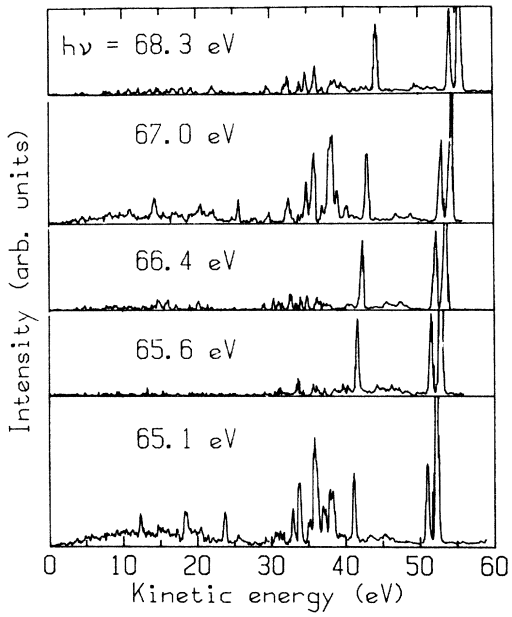

FIG. 5. Sequence of resonant (65.1, 67.0, and 68.3 eV) and nonresonant photoelectron spectra taken at several energies in the range of the $4d \rightarrow np$ excitations.

seen for the $5s$ and $5p_{1/2}$ lines in Fig. 5. This insensitivity of the main photoelectron lines to the discrete resonances is the key point of the next subsection.

C. Direct recombination of the $4d$ hole

Direct recombination of a core hole is the process in which the excited electron refills the core hole or leaves the atom. This process (involved transition) is also referred to as autoionization into the main lines because the final states reached are the nonresonant photoemission main lines. In the case of Xe below the $4d$ threshold we are dealing with $4d^9 5s^2 5p^6 np \rightarrow 4d^{10}(5s+5p)^7 \epsilon l$ transitions.

The relative oscillator strength into the main-line channels is a direct measure of the interaction of the excited Rydberg electron with the core hole and the valence electrons and therefore tells us something about the localization of this highly excited electron. Excitations to orbitals of Rydberg character tend to decay via resonant-Auger processes[27] corresponding to spectator satellite enhancement and resonant shakeoff processes. Because we have already seen qualitatively the predominance of the latter processes in the preceding subsection, the question arises as to the amount of decay via direct recombination. To address this question, we have taken spectra of the $5p$ and $5s$ main lines in small steps in the resonance region. Figure 6 shows the pronounced effect of the resonances on the $5p_{3/2}$:$5p_{1/2}$ branching ratio. In contrast to the branching ratio, the partial cross sections can be less affected, as seen in Fig. 7. This is in qualitative agreement with earlier but less detailed measurements.[24]

A quantitative analysis of the Fano-type profiles[28] of these partial cross sections was performed using the Fano theory modified for partial cross sections.[29,30] The application of this theory to photoemission experiments has been explained in considerable detail by Kobrin *et al.*[31] and Lindle *et al.*[32] and will be only briefly reviewed. Special emphasis will be placed on the problem of how to apply the theoretical approach to nearly Lorentzian absorption profiles and on the importance of interchannel coupling among the continuum channels within this framework.

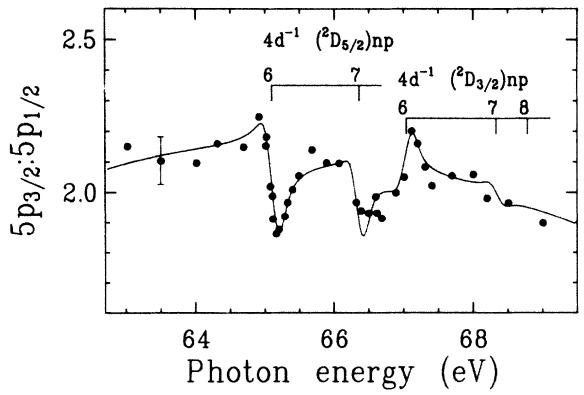

FIG. 6. $5p_{3/2}$:$5p_{1/2}$ branching ratio in the energy range of the $4d \rightarrow np$ excitations.

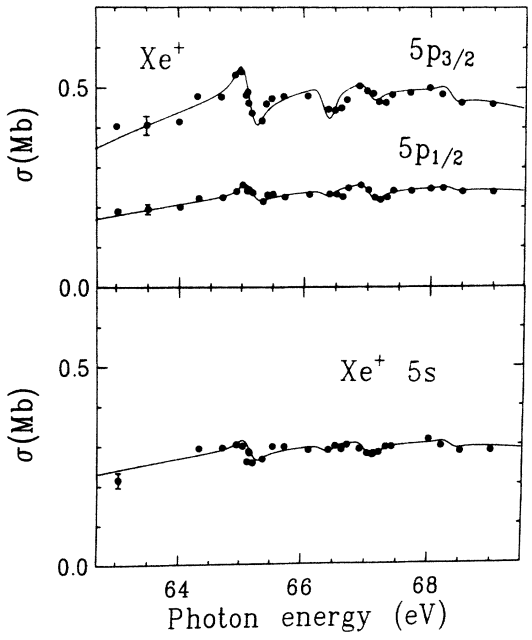

FIG. 7. (a) Partial cross sections of the spin-orbit components of the $5p$ photoline between 63 and 70 eV. (b) Partial cross section of the $5s$ photoline in the same energy region.

The curves drawn in Figs. 6 and 7 represent fits of Shore-type profiles and ratios of Shore-type profiles to the data, respectively. A Shore-type profile[33] is a differently parametrized Fano-type profile. In this parametrization the partial cross section for a sequence of n noninteracting resonances may be written as

$$\sigma(E)=\sum_{k=1}^{n}\frac{B_k+A_k\epsilon_k}{1+\epsilon_k^2}+C(E') \tag{1}$$

with

$$\epsilon_k=\frac{E-E_k}{\Gamma_k} \quad \text{and} \quad E'=E-E_1 ,$$

where E is the photon energy, Γ is the resonance widths, and A and B are characteristic constants of the corresponding resonance k which are related to the usual Fano parameters q and ρ^2 of an absorption spectrum. In absorption, these parameters are directly proportional to the interaction matrix element $\langle \Phi \mid V \mid \mu \rangle$ between the excited discrete state Φ and the continuum state μ and the dipole matrix elements between these two states and the ground state g. However, simple relations do not exist for partial cross sections because the observable photoemission channels are not equivalent with the prediagonalized states of the Fano theory. Upon transformation of these states, a general expression can be derived for the behavior of a partial cross section $\sigma_\mu(\epsilon)$ in the vicinity of an autoionizing resonance:

$$\sigma_\mu(\epsilon)=\sigma_0\left|\left[1+\alpha_\mu\left[\frac{q+i}{\epsilon-i}\right]\right]\right|^2 . \tag{2}$$

The sign convention used here follows the paper of Starace[29] and is inverse to the sign convention of Combet Farnoux.[30]

The parameter α_μ represents the fraction of the dipole amplitude $\langle g \mid r \mid \mu \rangle$ that passes through the eigenchannel μ and interacts with the discrete state:

$$\alpha_\mu = \frac{\langle \Phi \mid V \mid \mu \rangle}{\langle g \mid \mathbf{r} \mid \mu \rangle} \left[\frac{2\pi}{\Gamma} \sum_\mu \langle g \mid \mathbf{r} \mid \mu \rangle \langle \mu \mid V \mid \Phi \rangle \right] . \quad (3)$$

α_μ is in general a complex number because the effective interaction matrix element $\langle \Phi \mid V \mid \mu \rangle$ is actually a sum over the components of the observable photoelectron channel in terms of the prediagonalized continuum channels (Fano channels). These components are complex due to eigenchannel phase shifts resulting from the interaction among the observable channels. Without this interaction referred to as first-order interchannel coupling, the α parameter becomes a real number because the phase shift for all channels is constant. A general problem with this approach is the fact that each observable photoelectron channel consists of degenerate subchannels with different angular momenta. This difficulty allows the evaluation of individual matrix elements and partial decay rates only in special cases such as s-subshell photoionization. Even in this case, additional information on the angular distribution of the outgoing photoelectrons is necessary in order to quantitatively relate the squared average of the radial matrix elements to the average of the squared matrix elements which are related by the Schwartz inequality:

$$\mathrm{Re}\langle \alpha_\mu \rangle^2 + \mathrm{Im}\langle \alpha_\mu \rangle^2 \leq \langle \mid \alpha \mid^2 \rangle_\mu . \quad (4)$$

For Xe, there are two additional problems with this approach.

(1) The absorption spectrum shows highly symmetric Lorentzian-like line profiles,[7,12] corresponding to a large but not accurately known q value. Formula (1) depends on this absorption parameter q giving rise to large uncertainties.

(2) The modulations in the $5s$ channel due to the $4d \rightarrow np$ resonances are the weakest compared to the other channels, including the $5p$. Therefore, the $5s$ channel is not the channel best suited for a quantitative analysis, although in principle it is the most tractable. In order to cope with these problems, the basic relations describing autoionization were analyzed with respect to the special case of large q and small s-channel contribution. The key goals of such an analysis are to determine the order of magnitude of the imaginary parts of Eq. (1) and to reduce or eliminate the q dependence from this equation.

Using the Shore parametrization and the Schwartz inequality in the form

$$(\mathrm{Re}\langle \alpha \rangle_\mu)^2 + (\mathrm{Im}\langle \alpha \rangle_\mu)^2 = \gamma \langle \mid \alpha \mid^2 \rangle_\mu \quad (5)$$

with $0 \leq \gamma \leq 1$, one finds for $\mathrm{Re}\langle \alpha \rangle_\mu$ and $\mathrm{Im}\langle \alpha \rangle_\mu$

$$\mathrm{Re}\langle \alpha \rangle_\mu = \frac{\gamma + \frac{q}{2}\frac{A}{C} \pm \left[\gamma(\gamma-1) + \gamma \left[\frac{B}{C} + 1 \right] - \left[\frac{A}{2C} \right]^2 \right]^{1/2}}{q^2+1} ,$$
$$\mathrm{Im}\langle \alpha \rangle_\mu = q\,\mathrm{Re}\alpha - \frac{1}{2}\frac{A}{C} . \quad (6)$$

Neglecting all terms of order $1/q^2$ gives

$$\mathrm{Re}\langle \alpha \rangle_\alpha \approx \frac{1}{2q}\frac{A}{C} . \quad (7)$$

This approximation is quite good for Xe $4d \rightarrow 6p$ with a q value of $q \sim 200$.[7] Substituting this approximation in the expression for $\mathrm{Im}\langle \alpha \rangle_\mu$ yields $\mathrm{Im}\langle \alpha \rangle_\mu = 0$ for all channels in contrast to the general case of asymmetric absorption profiles.[31,32] This reduces the partial cross-section equation for a channel μ containing N degenerate final states to

$$\sigma_\mu(\epsilon) = \frac{\sigma_\mu^0}{1+\epsilon^2}[\epsilon^2 + 2\epsilon q\langle \alpha \rangle_\mu + 1 - 2\langle \alpha \rangle_\mu + (q^2+1)\langle \alpha^2 \rangle_\mu]$$
$$= \frac{\sigma_\mu^0[2q\langle \alpha \rangle_\mu \epsilon + (q^2+1)\langle \alpha^2 \rangle_\mu - 2\langle \alpha \rangle_\mu]}{1+\epsilon^2} + \sigma_\mu^0 . \quad (8)$$

This corresponds to a Shore parametrization yielding the following average α parameter in terms of the Shore parameters A, B, and C:

$$\langle \alpha \rangle_\mu = \frac{1}{2q}\frac{A}{C} \quad \text{and} \quad \langle \alpha^2 \rangle_\mu = \frac{1}{q^2+1}\left[\frac{B}{C} + \frac{A}{C}\frac{1}{q} \right] . \quad (9)$$

We see that in the case of nearly Lorentzian absorption profiles $\langle \alpha \rangle_\mu$ depends on the relative asymmetric modulation amplitude A/C, whereas the average $\langle \alpha^2 \rangle_\mu$ depends only on the Lorentzian part B/C of the modulation amplitude of the cross section $\sigma_\mu(\epsilon)$, to first approximation. The average of the squared α parameter still depends on the q value in the above approximation. To eliminate this dependence we determine the resonance enhancement factor for the resonance position $\epsilon = 0$ by the Fano formula

$$\rho^2(q^2-1) = \frac{\sigma_t(\epsilon=0) - \sigma_t}{\sigma_t} . \quad (10)$$

This relation remains valid even in the asymptotic case of a Lorentzian line profile. Further, we use the sum rule for the averages of the squared α parameters for all channels μ,

$$\sum_\mu \frac{\sigma_\mu^0}{\sigma_t} \langle \mid \alpha \mid^2 \rangle_\mu = \rho^2 , \quad (11)$$

which is equivalent to the sum rule for the partial decay widths Γ_μ/Γ:

$$\frac{\Gamma_\mu}{\Gamma}=\frac{\sigma_\mu^0}{\sigma_t}\frac{\langle|\alpha|^2\rangle_\mu}{\rho^2}=\frac{\sigma_\mu^0(q^2-1)\langle|\alpha|^2\rangle_\mu}{\sigma_t(\epsilon=0)-\sigma_t}\ . \tag{12}$$

Now we are able to write the partial decay width for an arbitrary channel μ with N degenerate final states for large q values directly in terms of the fitting parameters A, B, and C:

$$\frac{\Gamma_\mu}{\Gamma}=\frac{\sigma_\mu^0\left[\frac{B}{C}+\frac{1}{q}\frac{A}{C}\right]}{\sigma_t(\epsilon=0)-\sigma_t}\approx\frac{B}{C}\frac{\sigma_\mu^0}{\sigma_t(\epsilon=0)-\sigma_t}$$

$$=\frac{B}{\sigma_t(\epsilon=0)-\sigma_t}\ . \tag{13}$$

This equation gives Γ_μ/Γ primarily as the Lorentzian part B of the modulation amplitude of the partial cross section σ_μ relative to the total resonance enhancement at the resonance position. The contribution of the asymmetric part A to the partial decay width Γ_μ is suppressed by a factor proportional to the absorption value for q, here equal to ~ 200. Therefore, the partial decay width Γ_μ becomes in this case approximately equivalent to a "relative excess transition probability" due to the discrete state Φ, which also measures the symmetric part of the modulation of the cross section only.[28]

Table I gives the Shore parameters for the $5s$ and $5p$ channels at the first and strongest resonance, together with the partial decay widths derived from them using

TABLE I. Shore parameters A, B, and C and partial decay widths Γ_μ/Γ of the Xe $5s$ and $5p$ photoemission channels for the $4d_{5/2}\rightarrow 6p$ resonance.

Photoelectron channel	A [Mb]	B [Mb]	C [Mb]	Γ_μ/Γ%
$5s$	−0.1	0.01	0.285	0.07
$5p$	−0.287	0.054	0.686	0.4

$\sigma_t(\epsilon=0)=14.18$ Mb and $\sigma_t=1.15$ Mb.[7] We see that direct recombination contributes less than half a percent to the total decay rate of the $4d\rightarrow 6p$ excitation. The order of magnitude of our result is consistent with absorption and ion-yield measurements. This extremely small value shows the delocalized, diffuse character of the $6p$ Rydberg electron.

Such Rydberg electrons tend to hybridize easily with extended substrate electrons when the rare gas is absorbed on a metal substrate. This allows the excited electron to hop into the metal before the atomic Auger process occurs. As a consequence, the subsequent decay of the $4d$ hole would be in the absence of any excited-electron, normal d^{-1} Auger decay yielding N-00 Auger lines with constant kinetic energy instead of resonantly enhanced spectator satellites as in the free atom. This effect has been observed by Eberhard and Zangwill[34] for the Xe $4d\rightarrow np$ resonances in Xe on Cu metal and discussed by Wendin[35] in the context of many-electron effects.

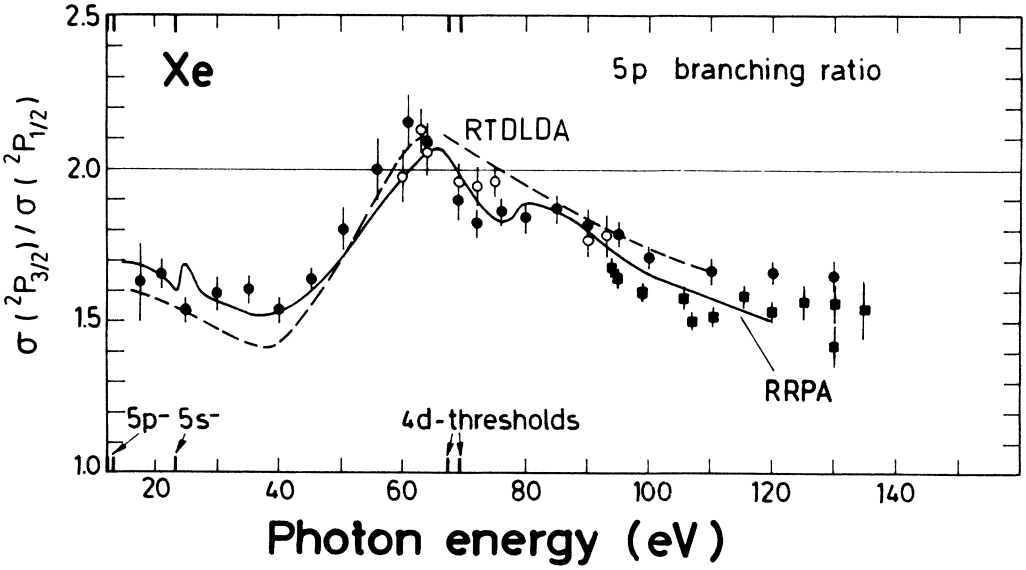

FIG. 8. $5p_{3/2}$:$5p_{1/2}$ branching ratio between 17 and 135 eV (closed and open circles and closed squares represent different sets of data). The theoretical curves are a RRPA calculation by Huang *et al.* (Ref. 36) and a RTDLDA calculation by Parpia and Johnson (Ref. 38).

D. The $5p_{3/2}$:$5p_{1/2}$ branching ratio

The broad energy-range behavior of the $5p_{3/2}$:$5p_{1/2}$ branching ratio outside the $4d \rightarrow np$ resonances is determined by the coupling between the $4d$ and $5p$ channels. The RRPA (Ref. 36) has taken into account this intershell coupling and describes the intensity sharing between these two channels in very good agreement with the experiment.[37] This theory predicts an additional dip around 75 eV (Fig. 8). Our data seem to indicate a small dip close to the $4d$ threshold. The difference in energy is probably due to the overly high $4d$ threshold energy used in the calculations. For comparison Fig. 8 also shows a relativistic time-dependent local density approximation (RTDLDA) calculation by Parpia and Johnson.[38] A further RRPA calculation for the Xe $4d_{5/2}$:$4d_{3/2}$ branching ratio[39] could also be confirmed[8] in good agreement with very recent measurements of Yates *et al.*[40] All these results in general prove the capability of the RRPA to describe the $5p$ and $4d$ photoionization process over a wide energy range in considerable detail.

In conclusion, we have shown that resonant shakeoff processes are important decay modes of the $4d \rightarrow np$ excitations. There are indications that shakeoff also participates significantly in the decay of the shape resonance above threshold. We have studied the direct recombination of the $4d$ hole (autoionization into the $5s$ and $5p$ main lines) in sufficient detail to derive quantitative partial decay widths. Application of the modified Fano theory for partial cross sections yields less then 0.5% for the contribution of direct recombination to the total decay rate of the $4d$ hole state, showing the Rydberg character of the excited np electrons.

ACKNOWLEDGMENTS

We thank A. Vinogradov (Leningrad State University) for his help in the measurements, D. Szostak for his assistance in the data analysis, and D. W. Lindle for critical reading of the manuscript. We would like to acknowledge technical assistance by the staff of the Hamburger Synchrotronstrahlungslabor at Deutsches Elektronen-Synchrotron (DESY) where this work was performed. It was supported by the Bundesministerium für Forschung und Technologie (Bonn, Federal Republic of Germany).

*Present address: Boehringer Mannheim G.m.b.H., D-6800 Mannheim 31, Federal Republic of Germany.

[1]A. F. Starace, in *Corpuscles and Radiation in Matter I,* Vol. 31 of *Handbuch der Physik,* edited by W. Mehlhorn (Springer, Berlin, 1982), p. 1.

[2]J. A. R. Samson, in Ref. 1, p. 123.

[3]K. T. Cheng and W. R. Johnson, Phys. Rev. A **28**, 2820 (1983); K. T. Cheng and C. Froese-Fischer, *ibid.* **28**, 2811 (1983).

[4]J. W. Cooper, Phys. Rev. Lett. **13**, 762 (1964).

[5]J. L. Dehmer, A. F. Starace, U. Fano, J. Sugar, and J. W. Cooper, Phys. Rev. Lett. **26**, 1521 (1971).

[6]R. Bruhn, E. Schmidt, H. Schröder, B. Sonntag, A. Thevenon, G. Passereau, and J. Flamand, Nucl. Instrum. Methods **208**, 771 (1983).

[7]D. L. Ederer and M. Manalis, J. Opt. Soc. Am. **65**, 634 (1975).

[8]E. Schmidt, H. Schröder, B. Sonntag, H. Voss, and H. E. Wetzel, J. Phys. B **18**, 79 (1985); E. Schmidt, thesis, Universität Hamburg, 1985.

[9]W. Gudat and C. Kunz, in *Synchrotron Radiation,* Vol. 10 of *Topics in Current Physics,* edited by C. Kunz (Springer, Berlin, 1979), p. 55.

[10]M. Y. Adam, F. J. Wuilleumier, N. Sandner, S. Krummacher, V. Schmidt, and W. Mehlhorn, Jpn. J. Appl. Phys. **17**, 170 (1978).

[11]A. Fahlmann, M. O. Krause, M. A. Carlson, and A. Svensson, Phys. Rev. A **30**, 812 (1984).

[12]T. Hayaishi, Y. Morioka, Y. Kageyama, M. Watanabe, I. H. Suzuki, A. Mikuni, G. Isoyama, S. Asaoka, and M. Nakamura, J. Phys. B **17**, 3511 (1984).

[13]R. Haensel, G. Keitel, P. Schreiber, and C. Kunz, Phys. Rev. **188**, 1375 (1969).

[14]M. J. Van der Wiel and T. N. Chang, J. Phys. B **11**, L125 (1978).

[15]U. Becker, R. Hölzel, H.-G. Kerkhoff, B. Langer, D. Szostak, and R. Wehlitz, in *Abstracts of Contributed Papers, Fourteenth International Conference on the Physics of Electronic and Atomic Collisions, Palo Alto, 1985,* edited by M. J. Coggiola, D. L. Huestis, and R. P. Saxon (ICPEAC, Palo Alto, 1985), p. 12.

[16]M. M. Hecht and I. Lindau, Phys. Rev. Lett. **47**, 821 (1981).

[17]G. R. Wight and M. J. Van der Wiel, J. Phys. B **10**, 601 (1977).

[18]C. E. Moore, *Atomic Energy Levels, Vol. III,* Natl. Bur. Stand. (U.S.) Circ. No. 467 (U.S. GPO, Washington, D.C., 1958).

[19]Th. M. El-Sherbini and M. J. Van der Wiel, Physica **62**, 119 (1972).

[20]J. B. West, P. R. Woodruff, K. Codling, and R. G. Houlgate, J. Phys. B **9**, 407 (1976).

[21]M. Ya. Amusia, V. K. Ivanov, and L. V. Chernysheva, Phys. Lett. **59A**, 191 (1976); M. Ya. Amusia and V. K. Ivanov, *ibid.* **59A**, 194 (1976).

[22]W. Eberhard, G. Kalkoffen, and C. Kunz, Phys. Rev. Lett. **41**, 156 (1978).

[23]V. Schmidt, Appl. Opt. **19**, 4080 (1980).

[24]S. Southworth, U. Becker, C. M. Truesdale, P. H. Kobrin, D. W. Lindle, S. Owaki, and D. A. Shirley, Phys. Rev. A **28**, 261 (1983).

[25]P. A. Heimann, D. W. Lindle, T. A. Ferrett, M. N. Piancastelli, and D. A. Shirley, in *Abstracts of Contributed Papers, Fourteenth International Conference on the Physics of Electronic and Atomic Collisions, Palo Alto, 1985,* edited by M. J. Coggiola, D. L. Huestis, and R. P. Saxon (ICPEAC, Palo Alto, 1985), p. 10.

[26]U. Becker, R. Hölzel, H.-G. Kerkhoff, B. Langer, D. Szostak, and R. Wehlitz, BESSY Annual Report 1984, 121 (1985).

[27]J. M. Bizau, P. Gérard, F. J. Wuilleumier, and G. Wendin, Phys. Rev. Lett. **22**, 2083 (1984).

[28]U. Fano, Phys. Rev. **124**, 1866 (1961); U. Fano and J. W. Cooper, *ibid.* **137**, A1364 (1965).

[29]A. F. Starace, Phys. Rev. A **16**, 231 (1977).

[30]F. Combet Farnoux, Phys. Rev. A **25**, 287 (1982).
[31]P. H. Kobrin, U. Becker, S. Southworth, C. M. Truesdale, D. W. Lindle, and D. A. Shirley, Phys. Rev. A **26**, 842 (1982).
[32]D. W. Lindle, T. A. Ferrett, U. Becker, P. H. Kobrin, C. M. Truesdale, H.-G. Kerkhoff, and D. A. Shirley, Phys. Rev. A **31**, 714 (1985).
[33]B. W. Shore, Phys. Rev. **171**, 43 (1968).
[34]W. Eberhard and A. Zangwill, Phys. Rev. B **27**, 5960 (1983).
[35]G. Wendin, Comments At. Mol. Phys. (to be published).
[36]K.-N. Huang, W. R. Johnson, and K. T. Cheng, At. Data Nucl. Data Tables **26**, 33 (1981).
[37]F. J. Wuilleumier, M. Y. Adam, P. Dhez, N. Sandner, V. Schmidt, and W. Mehlhorn, Phys. Rev. A **16**, 646 (1977); M. O. Krause, T. A. Carlson, and P. R. Woodruff, *ibid.* **24**, 1374 (1981).
[38]F. A. Parpia and W. R. Johnson, J. Phys. B **17**, 531 (1984).
[39]K. T. Cheng and W. R. Johnson, Phys. Rev. A **28**, 2830 (1983).
[40]B. W. Yates, K. H. Tan, L. L. Coatsworth, and G. M. Bancroft, Phys. Rev. A **31**, 1529 (1985).